RECENT PROGRESS IN IMPEDANCE MITIGATION FOR HL-LHC BEAM INSTRUMENTATION

M. Neroni*, W. Andreazza, R. Calaga, W. Hofle, I. Karpov, G. Khatri, M. Krupa, L. Margerison, M. McLean, C. Pasquino, H. Pommerenke, J. Storey, C. Vollinger
CERN, Geneva, Switzerland

Abstract

In the High-Luminosity LHC (HL-LHC) era, increased beam intensities and brightness impose stringent requirements on the beam-coupling impedance of accelerator components. This contribution summarizes recent studies on impedance mitigation for several new devices to be installed in the framework of the HL-LHC upgrades, illustrating design optimizations based on results from electromagnetic simulation solvers. Examples include the optimized design for crab cavity pick-ups and beam gas ionization profile monitors. These developments contribute to a consistent impedance mitigation strategy that reduces beam-induced heating at high intensities, maintaining device functionality and beam stability in the HL-LHC era.

INTRODUCTION

In preparation for the High-Luminosity LHC (HL-LHC) upgrade, the request for increased beam intensities, while maintaining beam quality poses stringent constrains on the overall beam coupling impedance. Minimising beam-induced heating is essential to preserve device integrity and performance, and it can be achieved by reducing the real part of the impedance. The total power loss is related to the beam intensity and beam coupling impedance through the following formula [1]:

$$P_{\text{loss}} = (f_{\text{rev}} e N_{\text{beam}})^2 \sum_{l=-\infty}^{\infty} |\Lambda(l\omega_{\text{rev}})|^2 \, \text{Re}[Z(l\omega_{\text{rev}})], \quad (1)$$

where f_{rev} is the revolution frequency and the total beam intensity is included in the term eN_{beam}, with e particle charge and N_{beam} accounting for the total number of bunches. The Fourier transform of the total beam distribution is the normalized beam spectrum, $\Lambda(\omega_{\text{rev}})$.

At the same time, it must be ensured that any additional source of beam coupling impedance does not significantly impact the beam stability threshold. In the longitudinal plane, it was observed that broadband impedance sources can reduce the coupled-bunch instability threshold below the one of loss of Landau-damping (LLD) [2]. The LLD threshold is inversely proportional to $\text{Im}(Z/n)$, with $n = f/f_{\text{rev}}$, ratio between the resonant and the revolution frequency. Therefore, keeping these contributions to a minimum is essential to avoid lowering the instability threshold.

Beam coupling impedance studies involve electromagnetic (EM) characterization of devices from the design phase prior to installation. Two mitigation examples are presented: the assessment of beam-induced heating in a beam gas ionization (BGI) profile monitor, and the impedance reduction for high-bandwidth beam position monitors (BPMs) as part of the HL-LHC crab cavities upgrade.

* michela.neroni@cern.ch

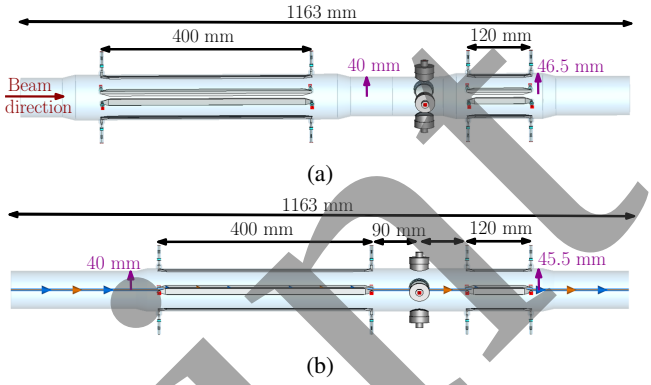

Figure 1: Initial (a) and final (b) geometry of high-bandwidth pick-ups used for intra-bunch measurements and for the crab cavity noise feedback and low-level RF system.

HIGH-BANDWIDTH BEAM POSITION MONITORS

In the framework of the HL-LHC project, combined-function BPMs (pick-ups) were developed to integrate a noise feedback system for the crab cavities and to provide head-tail beam diagnostics. The geometry (Fig. 1a) consists of 400 mm long striplines for intra-bunch measurements [3], followed by button pick-ups and 120 mm long striplines dedicated to the low-level RF system crab cavity noise feedback [4]. The inner surface of the stainless-steel beam pipe has a 10 μm copper coating to reduce resistive wall impedance. Below 50 MHz, even with the copper coating becoming transparent and the response being dominated by the conductivity of stainless steel, the impact on the overall beam coupling impedance remains negligible.

The pick-ups will be installed upstream and downstream of each crab cavity in IP1 and IP5, resulting in a total of four devices per beam. A beam coupling impedance assessment was performed prior to finalizing the design.

Longitudinal impedance simulations were performed with the CST wakefield solver [5]. All electrode feedthroughs were assumed to be impedance matched, as in the real system, to prevent undesired reflections within the structure. Figure 2 shows the resulting longitudinal impedance for the configuration illustrated in Fig. 1a. An oscillatory behaviour is observed up to 2 GHz, associated with the stripline length

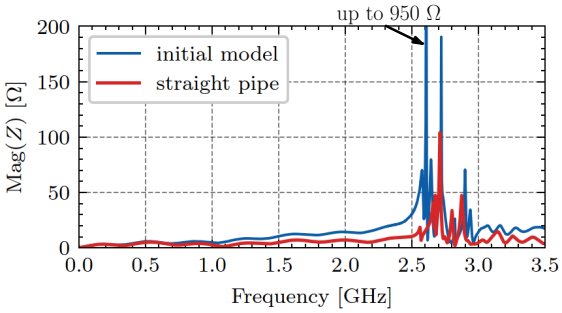

Figure 2: Longitudinal impedance from 1 MHz to 3.5 GHz: in blue for initial design of high-bandwidth BPMs and in red for the final design.

and consistent with the analytical expression reported in Ref. [6].

Above 2 GHz, a narrowband resonance is observed at 2.6 GHz with a shunt impedance of approximately 950 Ω. The electric field distribution for this resonance is represented in Fig. 3. A trapped transverse magnetic (TM) mode is located in the short (120 mm) stripline section. This part forms a cavity-like structure between two subsequent changes of beam pipe radius.

For impedance reduction, the primary objective was to eliminate radius variations and remove cavity-like volumes. A revised design with a constant radius of $r = 45.5$ mm was proposed, as shown in Fig. 1b. Simulations of the updated geometry demonstrate a significant impedance reduction (Fig. 2, red). The resonance at 2.6 GHz is completely suppressed and the maximum of the impedance magnitude is reduced to about 105 Ω at 2.71 GHz. Considering four BPMs per beam, the updated design contributes to a total effective $\mathrm{Im}(Z/n)$ of 0.05 mΩ that is lower compared to 0.07 mΩ for the initial design. This results in a negligible increase in effective $\mathrm{Im}(Z/n)$ relative to the current LHC impedance budget of 75 mΩ.

BEAM GAS IONIZATION PROFILE MONITOR (BGI)

The Beam Gas Ionization (BGI) profile monitor is a non-destructive beam instrumentation device for the measurement of the bunch-by-bunch transverse profile evolution throughout the acceleration cycle. In view of HL-LHC beam intensities, a new design has been developed [7]. The geometry, represented in Fig. 4, includes a steel cathode biased up to 30 kV. The overall structure is more compact than previous implementations in other accelerators, with the aim of reducing beam-induced heating and electromagnetic interference [8].

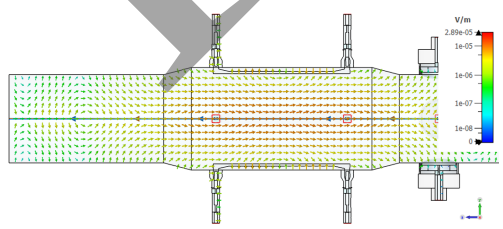

Figure 3: Electric field distribution at a frequency of 2.6 GHz. A trapped mode is observed in the beam pipe region where the radius transitions from 40 mm to a larger value of 46.5 mm, and then back to 40 mm.

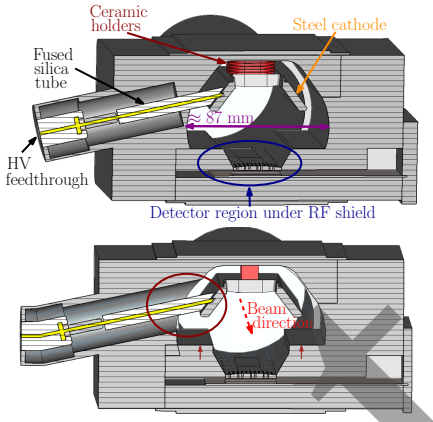

Figure 4: BGI monitor geometry: initial design (top) and impedance-optimised design (bottom), featuring an enlarged opening around HV pin, smaller ceramic holders, and raised shoulders near the RF shield.

Accurate electromagnetic modelling of the BGI requires identifying all relevant sources of resonances. In this case it was crucial to assess the impact of the high-voltage (HV) feedthrough. Figure 5 shows the real part of the impedance up to 2 GHz, comparing ideal matching at the feedthrough port (blue), a short circuit (green), and an open circuit (yellow). Without proper impedance matching, internal reflections introduce undesired resonances, as seen in the short and open circuit case.

In the current configuration, the inner HV pin is connected to the power supply through a 200 MΩ series resistor, resulting in a response similar to the open circuit case (Fig. 5, yellow). To reduce reflections and associated impedance contributions, a resistive termination matched to the feedthrough characteristic impedance ($Z_L \approx 44$) was proposed, with a series capacitor providing separation of DC and RF signal paths.

The longitudinal impedance trace is represented in black in Fig. 6, assuming a matched HV feedthrough. Two broadband ($Q \approx 1$) contributions can be identified at 169 MHz and at 882 MHz. Additional narrowband resonances are

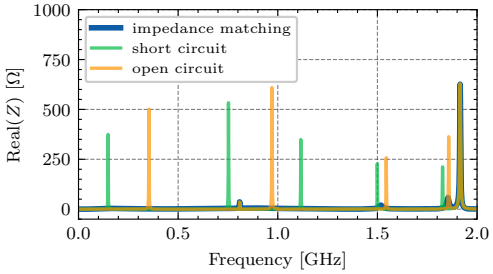

Figure 5: Real part of the longitudinal beam coupling impedance from 1 MHz to 2 GHz: matched HV feedthrough in blue, short circuit in green, and open circuit in yellow.

Table 1: Resonant frequency, quality factor and shunt impedance for narrowband resonances in the BGI before and after mitigation.

Before			After		
f_r [GHz]	Q_0	R_s [Ω]	f_r [GHz]	Q_0	R_s [Ω]
0.808	328	38	0.847	120	2
1.516	56	21.6	Broadband contribution left		
1.744	213	2.5	1.716	570	2.6
1.854	105	58	Broadband contribution left		
1.915	400	639	1.907	73	48

listed in Table 1 (left column) for the BGI before impedance mitigation. The beam-induced power loss was evaluated for the HL-LHC beam, assuming bunches with an intensity of $N_p = 2.3 \times 10^{11}$ p/b, a bunch length of 1 ns and a q-Gaussian distribution with $q = 0.6$ [9]. The normalized beam spectrum is represented in blue in Fig. 6. A worst-case statistical analysis, with resonant modes aligned to beam spectrum lines [10], yields a maximum total power loss of about 113 W. A power loss of 66 W originates from broadband contributions below 500 MHz. The power loss distribution shows that 98% of this power is passing through the HV feedthrough port. Consequently, a resistive load matching the characteristic impedance of the HV feedthrough must be incorporated to dissipate the extracted power. The residual power loss is caused by the impedance contribution from 500 MHz to 1.4 GHz, where a maximum of 46 W is reached when the resonant peak at 808 MHz aligns with the corresponding line of the beam spectrum.

Electric (E-) field monitors were implemented in simulation at the frequencies of interest to understand the location of the resonances. For the broadband contribution at 882 MHz, strong electric field enhancement was observed where the tank becomes narrower around the fused silica tube and the HV pin. The BGI design was modified with the introduction of a larger opening as indicated in the red circle in the geometry in Fig. 4 (bottom). This modification effectively suppresses the broadband impedance at 882 MHz as well as the resonances at 1.5 GHz and 1.85 GHz. Electric field monitors at the two major impedance peaks, 808 MHz and 1.91 GHz, are shown in Fig. 7. They indicated a similar E-field pattern, resembling a parallel-plate capacitor between the metallic cathode and the tank walls and enhanced by the ceramic holders. This effect can be interpreted as a parallel plate capacitor to ground, with a capacitance of approximately $C = (\varepsilon_R \varepsilon_0 A)/d$. The volume of the ceramic holders (macor, $\varepsilon_R = 6$) was reduced from 8.4 cm^3 to 2.2 cm^3 with the aim of obtaining a decrease of the equivalent ε_R in the gap. Additionally, the internal volume was reduced by increasing the height of the shoulders near the RF shield and detector region, as indicated by the red arrows in the geometry in Fig 4 (bottom).

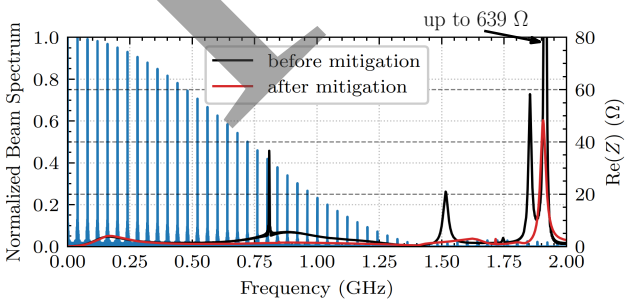

Figure 6: Normalized beam spectrum for HL-LHC beam parameters, in blue, real part of longitudinal impedance up to 2 GHz before (black) and after the mitigation (red).

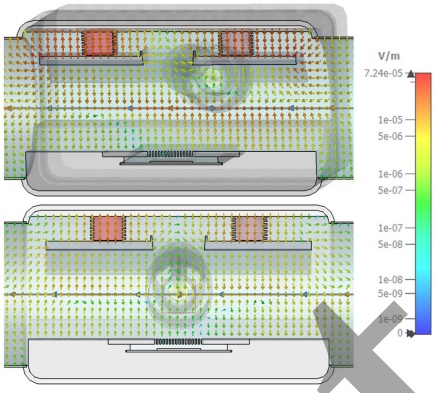

Figure 7: Electric field distribution showing a capacitive loading effect between the metallic cathode and the tank walls for resonances at 808 MHz (top) and 1.91 GHz (bottom).

The resulting real part of the impedance is shown in Fig. 6 (red). The impedance is significantly reduced in the relevant frequency range up to 2 GHz (Table 1, right column). The broadband contribution at 169 MHz remains untouched, causing the previously mentioned dissipated power of about 66 W. The shunt impedance at 1.91 GHz is reduced to 48 Ω, and the maximum total power loss decreases to 78 W. The proposed mitigation measures are currently under consideration, with a major focus on the matching network for the HV feedthrough.

CONCLUSION

The results presented highlight that impedance mitigation is essential to reduce beam-induced heating and to ensure component integrity with HL-LHC beams. It also aims to limit impedance sources that may lead to beam instabilities or reduced stability margins, with particular focus on the longitudinal broadband impedance to avoid lowering the LLD threshold. These results underline the need for a detailed understanding of the electromagnetic field distribution to identify resonances and define effective mitigation measures. Simple geometric modifications at the design stage can significantly reduce impedance contributions without affecting the primary functionality of the device. A beam stability assessment for the HL-LHC BGI will follow based on the finalised design. Impedance simulations will be validated by RF measurements before installation with the aim of benchmarking the electromagnetic model.

ACKNOWLEDGMENTS

The authors would like to express their gratitude to Heiko Damerau for the fruitful discussions.

REFERENCES

[1] M. Furman, H. Lee, and B. Zotter, "Energy Loss of Bunched Beams in RF Cavities", Lawrence Berkeley Laboratory, CA, USA, Rep. SSC-086, Aug. 1986.

[2] I. Karpov and E. Shaposhnikova, "Generalized threshold of longitudinal multibunch instability in synchrotrons", *Phys. Rev. Accel. Beams*, vol. 27, no. 7, p. 074401, Jul. 2024. doi:10.1103/PhysRevAccelBeams.27.074401

[3] M. Krupa, "EM stripline developments status and plans", unpublished. https://indico.cern.ch/event/1485774/

[4] R. Calaga and W. Hofle, "Conceptual Specification - BPTQR Crab Cavity RF Pick-up System", CERN, Geneva, Switzerland, Rep. LHC-BPM-ES-0015, 2024.

[5] CST Studio Suite, https://www.3ds.com/products-services/simulia/products/cst-studio-suite/

[6] K. Y. Ng, "Impedances of Stripline Beam Position Monitors", *Part. Accel.*, vol. 23, pp. 93–102, 1988.

[7] C. Pasquino *et al.*, "HL-LHC BGI mechanical design: integration, impedance and vacuum aspects", presented at IPAC'26, Deauville, France, May 2026, paper MOP1118, this conference.

[8] J. Storey *et al.*, "Beam Gas Ionisation (BGI) Profile Monitor: Status, Prospects and Risks", unpublished. https://indico.cern.ch/event/1585097/

[9] I. Zurbano Fernandez *et al.*, "High-Luminosity Large Hadron Collider (HL-LHC): Technical design report", *CERN Yellow Reports: Monographs*, vol. 10/2020, Dec. 2020. doi:10.23731/CYRM-2020-0010

[10] L. Sito, E. de la Fuente, F. Giordano, G. Rumolo, B. Salvant, and C. Zannini, "A Python Package to Compute Beam-Induced Heating in Particle Accelerators and Applications", in *Proc. HB'23*, Geneva, Switzerland, Oct. 2023, pp. 611–614. doi:10.18429/JACoW-HB2023-THBP52